STUCTURE AND CORRSION BEHAVIOR OF SPUTTER-DEPOSITED W-Mo ALLOYS

STUCTURE AND CORRSION BEHAVIOR OF SPUTTER-DEPOSITED W-Mo ALLOYS

Jagadeesh Bhattarai

Central Department of Chemistry, T.U.,
GPO Box 2040, Kathmandu, Nepal. E-mail: bhattarai_05@yahoo.com

Abstract:

Nanocrystalline, single bcc solid solutions of W-Mo alloys have been successfully prepared by D. C. magnetron sputtering in a wide composition. The corrosion behavior of the sputter-deposited W-Mo alloys was studied. The W-Mo alloys showed significantly high corrosion resistance in 12 M HCl at 30^{o} C. Their corrosion rates are about one and half orders of magnitude lower than that of sputter-deposited tungsten and lower than that of the sputter-deposited molybdenum even after prolonged immersion.

Introduction

The research activities on the sputter-deposited alloys are of widespread interest in the field of materials science during the last two decades. First, Nowak in 1976, has been reported that microcrystalline or amorphous coatings by sputtering greatly improved the corrosion resistance of stainless steel in aggressive solutions.[1] From the practical point of view, sputtering technique has been used as one of the appropriate methods for preparing highly corrosion-resistant single phase amorphous or nanocrystalline alloys during the periods of 1980,s.[2-6] The interesting finding of the lower corrosion rates of the sputter-deposited amorphous chromium-valve metal alloys[7-10] than those of the alloy-constituting elements encouraged to tailor new series of highly corrosion-resistant nanocrystalline molybdenum-valve metal alloys[11-14] and tungsten-valve metal alloys[15-34] by sputtering in recent years. In contrast to the sputter-deposited amorphous chromium- and tungsten-valve metal alloys, the sputter-deposited molybdenum-valve metal alloys were composed of a single phase nanocrystals, except amorphous Mo-Zr alloys. However, the sputter-deposited molybdenum-valve metal alloys showed higher corrosion resistance than those of alloy-constituting elements similarly to the sputter-deposited amorphous chromium- and tungsten-valve metal alloys in concentrated hydrochloric acids. One more step is pursued in this work to tailor corrosion-resistant binary W-Mo alloys by sputtering.

The main aims of this work are to characterize the structure of the sputter-deposited W-Mo alloys and to estimate their corrosion rate in 12 M HCl at 30^{o}C.

Experimental Methods

Preparation of W-Mo Alloys by Sputtering:

Direct current (D. C.) magnetron sputtering (SHIMADZU HSD-551S) was used to prepare specimens of binary W-Mo alloys on glass substrate. The sputtering machine used was installed in a clean room of class 5000 to avoid sources of the formation of defects in the deposits. The diagrammatic sketch of the D. C. magnetron sputtering is shown in **Figure 1**. The upper section of the diagram shows the cross-sectional view of the vacuum chamber of the sputtering machine. The vacuum chamber was composed of water-cooled three substrate holders and a target holder. The target of a 99.95% pure tungsten disc of 100 mm in diameter and about 6 mm in thickness was placed on the copper backing plate of the target holder which is shown lower section of the **Figure 1**. In addition, 99.95% pure molybdenum disc of 20 mm in diameter and about 3 mm in thickness was symmetrically placed on the sputter erosion region of the tungsten disc. For the purpose of homogenization of sputter-deposits, the substrate holder was revolved around the

central axis of the chamber, so that the substrates pass right above the target holder, in addition to revolution of the substrates themselves around their own axes. The composition of alloys was controlled by changing the numbers of disc of molybdenum on the tungsten target. The target holder was assembled of magnet, copper backing plate and the power source.

The vacuum chamber was evacuated to about 3-6 x 10^{-7} torr by using rotary and oil diffusion pumps after the target and the substrate were installed in the machine. When the above mentioned vacuum condition of the chamber was obtained, parameters such as rotation of the central axis of the substrate holder, rotation of three substrates, flow rate of argon, argon pressure in the chamber, and target ion current and voltage were controlled as tabulated in **Table 1**. Following pre-sputtering of the target for about 10-30 minutes for the purpose of removing contaminant oxide layers formed on the target surface, sputtering was carried out for about 3 hours at 4-9 x 10^{-4} torr of argon gas which was supplied after removal of oxygen, water and dust from 99.9995 % purity commercial argon gas. The target ion current of 0.5 A and the target voltage of 350-500 W were supplied during sputtering. The sputter-deposited W-Mo alloys were about 2 □m in thickness.

Preparation of Substrate:

The glass plate of 80 mm in length, 60 mm in width and 1.2 mm in thickness was used as substrate for sputter-deposition of all W-Mo alloys. Before the installation of the substrate to the sputtering chamber, glass plate was degreased by immersion in a 1 % (w/v) of commercial detergent solution for cleaning of aluminum metal at 75^{c} C for about 1 h, and then washed by boiling water and rinsed in de-ionized water. The cleaned glass substrate was dried by blowing hot air in sputtering room, and then installed in the substrate holder of the sputtering machine.

Structure of Alloys:

The structure of the sputter-deposited W-Mo alloys was confirmed by glancing incident X-ray diffractometer using a Rigaku Rotaflex RU-200B. The angle scanning mode was □□□where the X-ray incident angle (□) was fixed to 1^0. The angle scan rate was 2□degree /min (2 degree /min) with the sampling width of 0.02^0. The X-ray voltage of 40 kV and current of 150 mA were applied.

Apparent Grain Size of Alloys:

The apparent grain size of the prepared W-Mo alloys was estimated from the full width at half maximum (FWHM) of the most intense reflection in X-ray diffraction pattern using Scherrer,s formula as follows.[35]

$$t = 0.9 \quad / \quad \cos$$

where, t (nm) is apparent grain size, □ is the X-ray wavelength (= 0.15418 nm for Cu K□ radiation), □ is the full width at half maximum in radian (1 degree = □/ 180 radian) and □ is the diffraction angle of the most intense peak.

Composition of Alloys:

The composition of the sputter-deposited W-Mo alloys was determined using electron probe microanalysis (Shimadzu EPMA-Cl). The composition was determined three times from different portions of each alloy and average composition was estimated. The accelerating voltage of 15 kV and 15 nA of the sample current were applied. The composition of the sputter-deposited W-Mo alloys is summarized in **Table 2**.

Corrosion Test:

The corrosion test of the W-Mo alloys was conducted in 12 M HCl at 30^0C, open to air. Prior to corrosion test, the surface of specimens, which was cut into pieces having the area of about 20 cm^2, was polished mechanically with silicon carbide paper up to grit 1500 in cyclohexane, rinsed with acetone and hot air-dried. The corrosion rate of the alloys was estimated from the weight loss after immersion for 168 h in 12 M HCl at 30^0C. The weight of the specimen was recorded by using microbalance and the weight loss of the specimen was obtained from difference of weights of the specimen before and after immersion. The weight loss measurement for each alloys specimen was done two or three times and the average corrosion rate was estimated.

Results

Structure of Sputter-deposited W-Mo Alloys:

X-ray diffraction patterns of the sputter-deposited W-Mo alloys including sputter-deposited tungsten is shown in **Figure 2**. Alloy compositions hereafter are all denoted in atomic percentage (at %). For the sputtered tungsten, (110), (211 and (220) reflections of the bcc □-tungsten phase are clearly observed. The reflections of □-tungsten phase are also observed.[36,37] The W-Mo alloys are known to form a series of continuous bcc solid solutions at equilibrium at high temperatures as shown in **Figure 3**.[38] The sputter-deposited W-Mo alloys are not exceptional, and hence the W-Mo alloys can not be amorphized. All the sputter-deposited W-Mo alloys consist of a single bcc solid solution.

One of the characteristic features of the supersaturated solid solutions of the rapidly quenched binary alloys is the continuous change in the inter-atomic spacing of the alloys. In general, the inter-atomic spacing of the supersaturated solid solutions of the binary alloys varies almost linearly with concentration of the alloy element. From the X-ray diffraction patterns as shown in **Figure 2**, the most intense reflection of the sputter-deposited W-Mo alloys shifts continuously with concentration of molybdenum. To visualized this change, **figure 4** shows the change in the (110) lattice spacing as a function of the molybdenum content. The addition of molybdenum, with smaller Goldschmidt radius than tungsten, results in continuous decrease in the (110) spacing. The (110) spacing of W-Mo alloys changes continuously between the (110) lattice spacing of bcc tungsten and that of bcc molybdenum. Accordingly, all the sputter-deposited W-Mo alloys consist of a series of single bcc solid solutions by supersaturation of the alloying elements.

Though all the sputter-deposited tungsten alloys show a crystalline structure, broadening of the peak is clearly observed in **Figure 2**. Therefore, the apparent grain size of the sputter-deposited W-Mo alloys was estimated from the full width at half maximum (FWHM) of the most intense reflection using Scherrer,s formula.[35] **Figure 5** shows an example of the estimation of the apparent grain size of the W-24Mo alloy. For the sputter-deposited W-24Mo alloy, the diffraction angle of the most intense peak, that is, 2□ is equal to 40.32^0 . The full width at half maximum in degree is 0.435, and hence the value of □ (in radian) is equal to 0.0076 radians. Therefore, the calculated value of □cos□ is equal to 0.0071. The X-ray wavelength for Cu K□ radiation, that is, □ equal to 0.15418 nm, and hence the value of (0.9 x □) equal to 0.1387 nm. By substituting these values to the Scherrer,s formula as shown in **Figure 5**, it is obtained the value of 19.53 nm as an apparent grain size for the W-24Mo alloy. Similarly, the apparent grain size of all the sputter-deposited W-Mo alloys was estimated separately.

Figure 6 shows the change in the apparent grain size of the sputter-deposited W-Mo alloys as a function of molybdenum content. The apparent grain size of all the sputter-deposited W-Mo alloys including the sputter-deposited tungsten and molybdenum is less than 20 nm. Therefore, the sputter-deposited W-Mo alloys are supposed to be composed of nanocrystals. Consequently, the sputter-deposited W-Mo alloys consist of a series of supersaturated nanocrystalline single bcc solid solutions.

Corrosion Rate of W-Mo Alloys:

Figure 7 shows the change in corrosion rates of the sputter-deposited W-Mo alloys after immersion for 168 h in 12 M HCl at 30^oC, open to air. The corrosion rates of the sputter-deposited tungsten and molybdenum are also shown for comparison. The corrosion rate of the sputter-deposited tungsten and molybdenum are 2.5×10^{-2} mm y^{-1} and 3.9×10^{-2} mm y^{-1}, respectively, after immersion in 12 M HCl at 30^oC. The corrosion rate of the sputter-deposited W-Mo alloys decreases sharply with increasing molybdenum content and becomes almost constant when the alloy containing 24-69 at % molybdenum. The corrosion rates of the W-Mo alloys containing 24 at % or more molybdenum are about one and half orders of magnitude lower than that of tungsten and even lower than that of the sputter-deposited molybdenum. All these sputter-deposited W-Mo alloys, except W-9Mo alloy, which are composed of a nanocrystalline single bcc phase, show lower corrosion rates than those of alloy-constituting elements (that is, tungsten and molybdenum) in 12 M HCl at 30ºC.

Discussion

The W-Mo alloys can not be amorphized. All the sputter-deposited W-Mo alloys are composed of nanocrystalline bcc solid solutions. A number of methods have emerged that can be used for the prediction of the amorphization range of binary alloy systems.[39-43] It has been generally accepted that prerequisite conditions for amorphization of binary by rapid quenching are a large negative mixing enthalpy of alloying constituents[44,45], a lower atomic radius ratio of the alloy constituents than 0.85[44,46-48], the existence of a deep eutectic[49] and the alloying elements belonging to distance groups in Periodic Table.[44,46] The amorphization of W-Mo alloys is difficult because of the very low negative mixing enthalpy of – 1 kJ mol^{-1} [50] and the atomic size ratio of 1.01.[47] On the other hand, both the alloying elements of the W-Mo alloys belong to same groups in the Periodic Table. Consequently, W-Mo alloys do not satisfy the prerequisites conditions for amorphization of the alloys.

The sputter-deposited W-Mo alloys, which are composed of a nanocrystalline single bcc phase, show higher corrosion resistance than those of alloy-constituting elements in 12 M HCl at 30°C. It is already mentioned that the apparent grain size of the sputter-deposited W-Mo alloys is less than 20 nm, and hence the corrosion-resistant of the W-Mo alloys is higher than those of alloy-constituting elements. It can, therefore, be said that both tungsten and molybdenum improve the corrosion resistance of the alloys synergistically. The similar synergistic effect has been reported for the sputter-deposited tungsten-[15,19,23-26] and chromium[7-10]-valve metal (titanium, zirconium, niobium and tantalum) alloys in concentrated hydrochloric acids.

Conclusions

New series of highly corrosion-resistant W-Mo alloys are tailored by direct current (D. C.) magnetron sputtering. The structure of the sputter-deposited W-Mo alloys is characterized and their corrosion rate is estimated in 12 M HCl at 30°C. Following conclusions can be drawn;

1. A nanocrystalline single bcc solid solution of the sputter-deposited W-Mo alloys are successfully prepared in a wide composition range.
2. Corrosion rates of the sputter-deposited W-Mo alloys are lower than those of alloy-constituting elements, that is, sputter-deposited tungsten and molybdenum.

Acknowledgements

The author is thankful to Emeritus Prof. Dr. K. Hashimoto of the Tohoku University, Japan for his kind permission to use sputtering machine and electron probe microanalysis.

References

1. W. B. Nowak, *Mater. Sci. Eng.,* 1976, **23**, 301.
2. R. B. Diegle and M. D. Merz, *J. Electrochem. Soc*., 1980, **127**, 2030.
3. R. R. Ruf and C. C. Tsuei, *J. Appl. Phys*., 1983, **54**, 5705.
4. R. G. Walmesley et al., *J Non-Cryst. Solids*, 1984, **61-62(I)**, 625.
5. K. Shimamura et al., in *Proc. MRS Intl. Meeting on Advanced Materials*, Tokyo.**Vol.3**, MRS. Pittsburgh, Pennsylvania, 1988, p. 335.
6. W. C. Moshier et al*., J. Electrochem. Soc*., 1989, **136**, 356.
7. J. H. Kim et al., *Corros. Sci.,* 1992, **33**, 1507.
8. J. H. Kim et al., *Corros. Sci.,* 1993, **34**, 975.
9. J. H. Kim et al., *Corros. Sci*., 1993, **34**, 1817.
10. J. H. Kim et al., *Corros. Sci.,* 1993, **34**, 1947.
11. P.Y. Park et al., *Corros. Sci.,* 1995, **37**, 307.
12. P.Y. Park et al., *Corros. Sci.,* 1996, **38**, 397.
13. P.Y. Park et al., *Corros. Sci*., 1996, **38**, 1649.
14. P.Y. Park et al., *Corros. Sci*., 1996, **38**, 1731.
15. J. Bhattarai, E. Akiyama, A. Kawashima, K. Asami and K. Hashimoto, *Corros. Sci.,* 1995, **37**, 2071.
16. J. Bhattarai, E. Akiyama, A. Kawashima, K. Asami and K. Hashimoto, 1995, in *Proc. 42nd Japan Corros. Conf.*, Sapporo, Japan, **D-206**, 515.
17. J. Bhattarai, E. Akiyama, H. Habazaki, A. Kawashima, K. Asami and K. Hashimoto, in *Proc. JSCE Corrosion 96*, Japan Society of Corrosion Engineering, Tokyo, Japan, 1996, **B-203**, 175.

18. J. Bhattarai, E. Akiyama, H. Habazaki, A. Kawashima, K. Asami and K. Hashimoto, 1995, in *Proc. 43rd Japan Corros. Conf.*, Osaka, Japan**, D-207**, 419.
19. J. Bhattarai, E. Akiyama, H. Habazaki, A. Kawashima, K. Asami and K. Hashimoto, *Corros. Sci*., 1997, **39**, 355.
20. J. Bhattarai, E. Akiyama, H. Habazaki, A. Kawashima, K. Asami and K. Hashimoto, in *Proc. JSCE Corrosion 97*, Japan Society of Corrosion Engineering, Tokyo, Japan, 1997, **D-102**, 263.
21. J. Bhattarai, E. Akiyama, H. Habazaki, A. Kawashima, K. Asami and K. Hashimoto, 1997, *in Proc. 44th Japan Conf. Materials and Environments*, Sendai, Japan, **B-208**, 199.
22. J. Bhattarai, E. Akiyama, H. Habazaki, A. Kawashima, K. Asami and K. Hashimoto, 1997, *in Proc. 44th Japan Conf. Materials and Environments*, Sendai, Japan, **B-210**, 205.
23. J. Bhattarai, E. Akiyama, H. Habazaki, A. Kawashima, K. Asami and K. Hashimoto, *Corros. Sci*., 1998, **40**, 19.
24. J. Bhattarai, E. Akiyama, H. Habazaki, A. Kawashima, K. Asami and K. Hashimoto, *Corros. Sci.*, 1998, **40**, 757.
25. J. Bhattarai, E. Akiyama, H. Habazaki, A. Kawashima, K. Asami and K. Hashimoto, *Corros. Sci.*, 1998, **40**, 1897.
26. J. Bhattarai, *Tailoring of Corrosion-resistant Tungsten Alloys by Sputtering, Ph. D. Thesis*, Tohoku University, Japan, 1998, p. 1-229.
27. J. Bhattarai and K. Hashimoto, *Tribhuvan Uni. J.*, 1998, **21-2**, 1.
28. J. Bhattarai, *J. Nepal Chem. Soc.*, 2000, **19**, 1.
29. J. Bhattarai, *J. Nepal Chem. Soc*., 2000, **19**, 32.
30. J. Bhattarai, *J. Nepal Chem. Soc*., 2001, **20**, 24.
31. J. Bhattarai, *in 6th Intl. Asian Conf. On Analytical Sciences*, Tokyo, Japan, 2001, in abstract no. **2DI-05**, 47.
32. J. Bhattarai, *Nepal J. Sci. Technol*., 2002, **4**, 37.
33. J. Bhattarai, *J. Insti. Sci. Technol*., 2002, **12**, 125.
34. J. Bhattarai, *39th Intl. Symp. On Macromolecules*, Beijing, China, 2002, in abstract no. **9e-4p-19**, 581.
35. B. D. Cullity, *Elements of X-ray Diffraction*, 2nd edition, Addison-Wesley Publ. Company, Inc., USA, 1977, p.101.
36. B. C. Krebs et al., *z. anorg. allg. chem*. (in German), 1987, **553**, 127.
37. M. Kadri and A. Deneuville, *Mater. Sci. Eng*., 1988, **98**, 79.
38. T. B. Massalki et al., *Binary alloy Phase Diagram*, 2nd edition, ASM Intl. Materials Park, Oho, 1990.
39. M. H. Cohen and D. Turnbull, *Nature*, 1961, **189**, 131.
40. M. S. Chen and D. Turnbull, *J. Chem. Phys*., 1968, **48**, 2560.
41. I. W. Donald and H. A. Davies, *J. Non-Cryst. Solids*, 1978, **30**, 77.
42. S. H. Whang, *Mater. Sci. Eng.,* 1983, **57**, 87.
43. S. H. Whang, *J. Non-Cryst. Solids*, 1984, **61/62**, 841.
44. B. C. Giessen and S. H. Whang, *J. Phys. (Paris) Colloq*., 1980, **C8**, 95.
45. I. J. Polmear, *Mater. Trans. JIM*, 1996, **37**, 12.
46. T. Masumoto and R. Maddin, *Mater. Sci. Eng*., 1975, **29**, 1.
47. T. Egami and Y. Waseda, *J. Non-Cryst. Solids*, 1984, **64**, 113.
48. M. Li and W. L. Johnson, *Phys. Rev. Letts*., 1993, **70**, 1120.
49. J. W. Allen et al., *J. Non-Cryst. Solids*, 1980, 113.
50. A. K. Niessen et al., *Calphad*, 1983, **8**, 51.

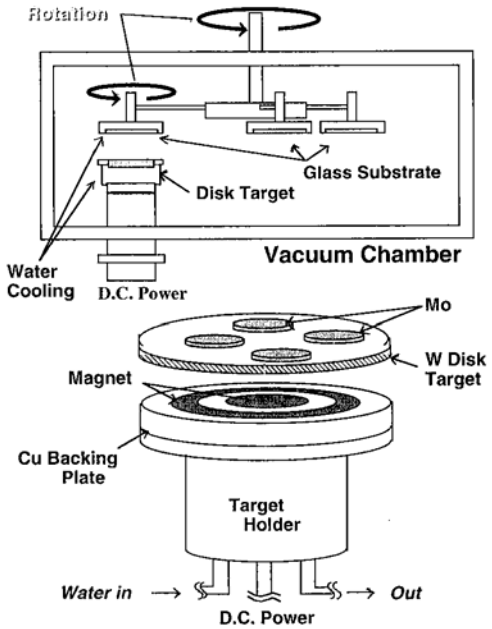

Figure 1. Diagrammatic sketch of the direct current (D.C.) magnetron sputtering.

Table 1. Parameters of vacuum chamber of the sputtering machine.

Rotation of substrate holder	4.65 rpm
Rotation of Substrates	14.6 rpm
Target-substrate spacing	5.0 cm
Flow rate of argon gas	5.0 ml/min
Vacuum pressure of chamber (before sputtering)	$3\text{-}6\times10^{-7}$ Torr
Argon pressure of chamber (During sputtering)	$4\text{-}9\times10^{-4}$ Torr
Target ion current/Voltage	0.5 A/350-500 W

Table 2. Chemical composition of the sputter-deposited W-Mo alloys.

Alloys' name	Molybdenum content (at %)	Tungsten content (at %)
W-9Mo	9.0	91.0
W-24Mo	24.2	75.8
W-34Mo	34.2	65.8
W-52Mo	51.8	48.2
W-69Mo	69.3	30.7
W-83Mo	82.8	17.2

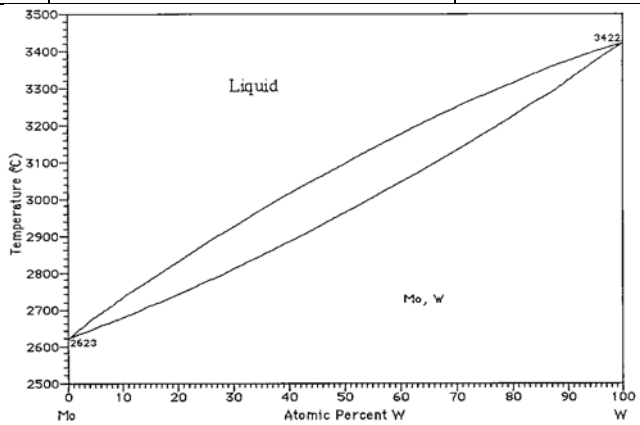

Figure 2. X-ray diffraction patterns of sputter-deposited W-Mo alloys including sputter-deposited tungsten.

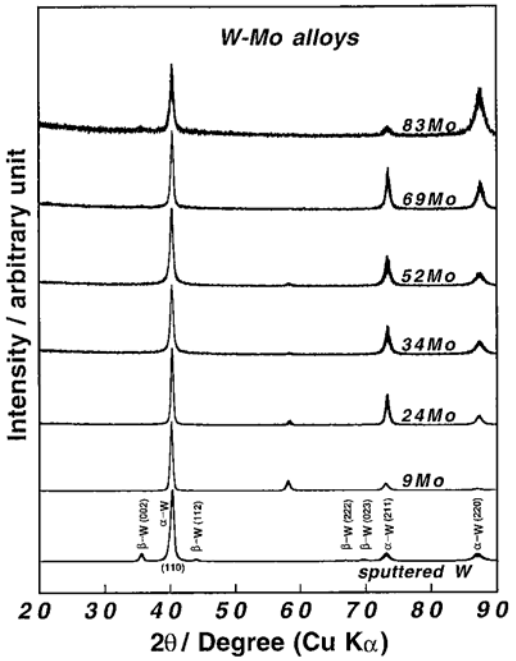

Figure 3. Phase diagram of W-Mo system (produced from Massalki et al., 38)

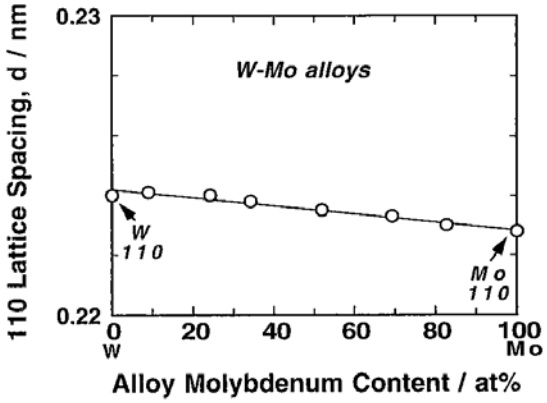

Figure 4. Change in the (110) lattice spacing of the sputter-deposited W-Mo alloys estimated from the most intense peak position in X-ray diffraction patterns as a function of molybdenum content of the alloys.

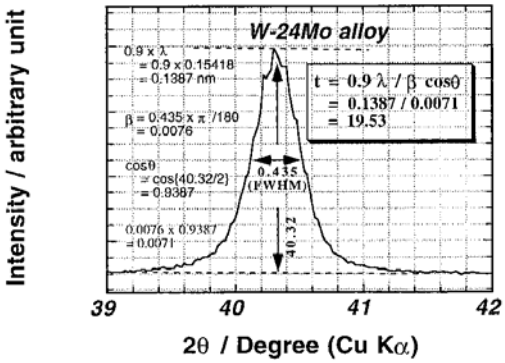

Figure 5. An example of the estimation of apparent grain size of sputtered W-24Mo alloy from the full width at half maximum of the most intense peak in X-ray diffraction pattern using Scherrer's formula.

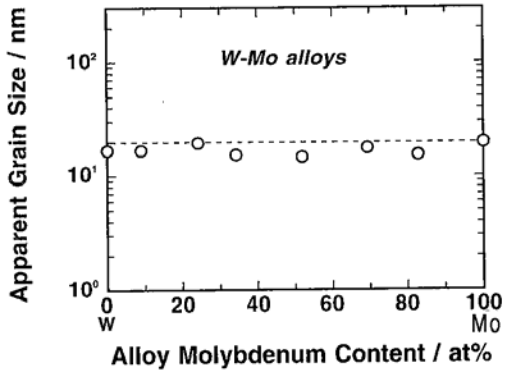

Figure 6. An estimated apparent grain size of sputter-deposited W-Mo alloys including sputter-deposited tungsten and molybdenum.

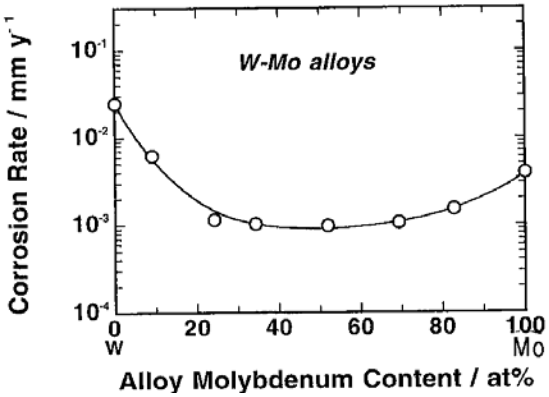

Figure 7. Corrosion rates of the sputter-deposited W-Mo alloys in 12 M HCl 30°C. The corrosion rates of the sputtered tungsten and molybdenum are also shown for comparison.